Smooth muscle Ca^{2+} sensitization causes hypercontractility of middle cerebral arteries in mice bearing the Familial Hemiplegic Migraine type 2 associated mutation.

AUTHORS: Christian Staehr[1], Lise Hangaard[1], Elena V. Bouzinova[1], Sukhan Kim[1], Rajkumar Rajanathan[1], Peter Boegh Jessen[1], Nathan Luque[3], Zijian Xie[2], Karin Lykke-Hartmann[1], Shaun L. Sandow[3], Christian Aalkjaer[1], Vladimir V. Matchkov[1]

[1] Department of Biomedicine, Aarhus University, Denmark

[2] Marshall Institute for Interdisciplinary Research, Marshall University, Huntington, WV, USA

[3] Faculty of Science, Health, Education and Engineering, University of the Sunshine Coast, Maroochydore, Qld, 4558, Australia

SUPPLEMENTARY INFORMATION

SUPPLEMENTARY METHODS

All experiments conformed to guidelines from the European Convention for the Protection of Vertebrate Animals used for Experimental and other Scientific Purposes and were approved by and conducted with permission from the Animal Experiments Inspectorate of the Danish Ministry of Environment and Food. Animal experiments were reported in accordance with the ARRIVE (Animal Research: Reporting *in vivo* Experiments) guidelines (www.nc3rs.org.uk/arrive-guidelines).

Atp1a2$^{+/-G301R}$ mice

The Atp1a2$^{+/-G301R}$ mice were generated by introduction of the G301R mutation in *Atp1a2* gene, as described previously.[1] Mice were housed under a 12:12 light/dark cycle, food and water were provided *ad libitum*. Breeding with two heterozygous Atp1a2$^{+/-G301R}$ mice resulted in homozygous, heterozygous and wild type (WT) pups, as standard;[1] with all pups being genotyped (forward primer: 5'-gag cag agc tga ctc aga agc at; reverse primer: 5'-gct tctcag cag tgt tct tcc ctt).

Homozygote pups died immediately after birth; resembling the lethal phenotype previously reported for other genetic disturbances in the *Atp1a2* gene.[2-4] Heterozygous Atp1a2$^{+/-G301R}$ (*n*=82) and WT (*n*=86) mice ~12-16 weeks old were used in the current study. A previous study found some sex-coupled differences in behavioural tests.[1] However, in the current study, an equal number of males and females were used, and as no sex-coupled difference was seen, and data from male and females were pooled in the final analyses. Final analysis was not blinded. Middle cerebral arteries and mesenteric small arteries from littermate Atp1a2$^{+/-G301R}$ and WT mice were used.

Quantitative Polymerase Chain Reaction (qPCR)

The RNA isolation was carried out with Qiagen micro kit (Qiagen, VWR, Denmark). Reverse transcription was executed with reverse transcriptase III (Invitrogen, Denmark) and superase (Ambion Ltd., UK) was used for deactivation of RNAse and DNAse. The qPCR was carried out on MX3000P (Stratagene, USA) using Taqman probe (FAM) technology. Gene expression was normalized to reference gene and presented as a ΔCt value. Comparison of gene expression was derived from subtraction of averaged WT ΔCt in the experiment from ΔCt value in the analysed probe (either WT or Atp1a2$^{+/-G301R}$), producing ΔΔCt. Relative gene expression was calculated as $2^{-\Delta\Delta Ct}$.

Primer set for qPCR analysis of the total Na,K-pump α2 isoform expression was obtained from Applied Biosystems, Denmark; Rn00560789 and Rn01533986. In the experiments where expressions of mutated and WT *Atp1a2* allele were distinguished, the primer set detecting the WT allele was only used (forward primer: 5'-aggggtggctgtgttcctgg; reverse primer: 5'-tccaggttcttcaccaggca; probe: 5'-ctcatcctgggctacagctggctggaggca). Glyceraldehyde 3-phosphate

dehydrogenase (GAPDH; forward primer: 5'- cacggcaagttcaacggcacag; reverse primer: 5'- agactccacgtcatactcagcacc; probe: 5'- agctggtcatcaacgggaaccccatcacca) was used as a reference gene.

Semi-quantification of cSrc and MYPT phosphorylation

Arterial segments were fixed in ice-cold 10 mM DL-Dithiothreitol (DTT) in acetone with 10% trichloroacetic acid and stored at -80°C for 8-10 hours. Arteries were then washed in ice-cold acetone with 10 mM DTT and lysed in SL mixture (in mM: Tris-HCl 10, sucrose 250, EDTA 1, EGTA 1; Triton X-100 2%, pH 7.4; 1 tablet protease inhibitor per 10 mL and 10^{-5} M of Halt's phosphatase inhibitor cocktail and 2x trisglycine sodium dodecyl sulfate buffer (Invitrogen, Denmark) with 1 M DTT). The homogenates were kept for 10 min at 95°C, ultrasonicated for 45 sec and centrifuged at 10,000 g. Note, that this procedure does not permit detection of the lysate protein concentration prior to gel loading.

Proteins were separated on 4-15% trisglycine gels and electrotransferred onto nitrocellulose membranes. Membranes for identification of phosphorylated proteins were blocked in 3% bovine serum albumin (BSA) in Tris-buffered solution (TBS: 10 mM Tris HCl, 100 mM NaCl, pH 7.6) with 0.5% vol/vol Tween 20 (TBST). Membranes for identification of total cSrc and MYPT proteins were blocked in 0.3% iBlock in TBS for 2 h. Membranes were cut at approximately 100 kDa, 50 kDa and 35 kDa, and the upper segment used for MYPT detection (expected band ~130 kDa), middle segment for cSrc detection (expected band ~65 kDa), and the lower segment for the house-keeping protein thioredoxin 2 detection (expected band ~12 kDa).

The membranes were incubated with primary antibodies (pY418 cSrc 1 : 200, Invitrogen [Catalog no. 44660G], diluted in 3% BSA in TBS; total cSrc 1 : 500, Santa Cruz Biotechnology Inc. [Catalog no. sc-8056], diluted in 0.3% iBlock in TBST; pT850 MYPT 1:500, Millipore [Catalog no. 04-773], diluted in 3% BSA in TBS; total MYPT 1:6,000, Santa Cruz Biotechnology Inc. [Catalog no. sc-25618], diluted in 0.3% iBlock in TBST; thioredoxin 2 1:10,000, Abcam [Catalog no. ab185544], diluted in 0.3% iBlock in TBST) overnight at +4°C. After washing, the membranes were incubated with horseradish-peroxidase-conjugated secondary antibody (1:2000; Dako, Denmark) for 1.5 hour in TBST. Excess antibody was removed by extensive rinsing, and bound antibodies detected by an enhanced chemiluminiscence kit (ECL, Amersham, UK).

Proteins (MYPT or cSrc) were semi-quantified by measuring band intensities using ImageJ software (NIH, USA). Protein phosphorylation were semi-quantified as a ratio between phospho-protein and total protein. The average measurements from WT group under resting conditions (i.e. in the absence of drugs) was set to 100% to compare the effects of drug interventions detected from the same gel. The total cSrc and MYPT protein expression was individually normalized to the corresponding band intensity of thioredoxin 2 from the same load, and semi-quantified by setting normalized intensity measured for WT group to 100%.

Whole-mount staining of arterial segments

Mice were deeply anesthetized with pentobarbital (150mg/kg; i.p.) and perfusion-fixed with 4% paraformaldehyde in phosphate-buffered saline (PBS, in mM: NaCl 137, KCl 2.7, Na_2HPO_4 8.2, KH_2PO_4 1.8, at pH 7.4), as described previously.[5] The brain and mesentery were removed and arteries dissected into PBS. After washing, tissues were incubated at room temperature for 2h in blocking buffer (1% BSA and 0.2% Triton in PBS), further washed and incubated overnight with primary antibody (α1, Alomone, ANP001, lot ANP001ANO102; α2, Millipore, AB9094, lot 2136593; NCX, Santa Cruz, sc-32881; all 1:100) in blocking buffer at 4°C, washed again and incubated in secondary antibody (Alexa Fluor 633, 1:200; Molecular Probes/Invitrogen, A21070; lot #50728A) in 0.1% Triton in PBS for 2 h at room temperature. Tissue was subsequently mounted in anti-fade mounting media; with the media of select preparations also containing 0.002% propidium iodide to clarify cell layer patency. Tissue was imaged with uniform confocal settings. Controls involved peptide block of primary antibody in a 1:10 (v/v) excess of the immunizing peptide; and secondary only was used as a 'zero' setting.

Isometric force measurement of isolated arteries

Mice were sacrificed by cervical dislocation, and the brain and mesentery dissected into ice-cold physiological salt solution (PSS; in mM: NaCl 115.8, KCl 2.82, KH_2PO_4 1.18, $MgSO_4$ 1.2, $NaHCO_3$ 25, $CaCl_2$ 1.6, EDTA 0.03, glucose 5.5, gassed with 5 % CO_2 in air and adjusted to pH 7.4). Arteries were cleaned of connective tissue in ice-cold PSS and mounted in a wire myograph (Danish Myo Technology A/S, Denmark) for isometric force measurements at 37°C. The artery diameter was set to a value where maximal active force is obtained.[6] Force (mN) was recorded with a PowerLab 4/25 – Chart7 acquisition system (ADInstruments Ltd., New Zealand) and converted to wall tension by dividing the force with two times the arterial segment length.

The study was performed on endothelium intact arteries, unless otherwise stated. In experiments, where endothelium was removed, an air bubble was passed through the arterial lumen for 1 minute prior to the arteries being mounted in the isometric myograph using a cannula, which was placed in the vessel opening. Successful removal of endothelium was demonstrated by a lack of acetylcholine (10^{-5} M) induced relaxation of a vessel pre-constricted to approximately 50% of maximal tone.

Simultaneous measurements of isometric force and $[Ca^{2+}]_i$

Ratiometric $[Ca^{2+}]_i$ measurements were obtained simultaneously with force measurements in a myograph. Arterial segments were loaded with 2.5 μM fura 2-acetoxymethyl ester dissolved in DMSO with 0.1% (wt/vol) cremophor and 0.02% (wt/vol) pluronic F127 for 2h. It has been previously shown that this loading protocol enables measurement of smooth muscle $[Ca^{2+}]_i$ with negligible contribution from endothelial cells.[7] Arteries were excited by a 75W xenon light source

alternately at 340 and 380 nm, and emitted light was measured at 515 nm. Background fluorescence (after quenching with 20 mM $MnCl_2$) was determined and subtracted from obtained measurements. Fluorescence was collected using Felix32 software (version 1.2, Photon Technology, USA). $[Ca^{2+}]_i$ was expressed as the ratio of fluorescence during excitation at 340 nm and 380 nm.

Simultaneous measurements of isometric force and membrane potential

Smooth muscle membrane potential in the intact vascular wall was measured in arteries mounted in an isometric myograph (Danish Myo Technology A/S, Denmark) using glass KCl-filled microelectrodes with resistance in the range of 40–100 MΩ as previously described.[8] A Ag-AgCl electrode in the organ bath was used as a reference. Electrode resistance was routinely compensated by balancing the Wheatstone bridge of the amplifier (Intra-767, WPI) before impalements. Membrane potential was averaged over 1 minute of recording, at least 1 minute after U46619 application.

Morphometric measurements

Arteries were mounted in a wire myograph in PSS and morphometric measurements performed using a light microscope (40x water immersion lens), as previously described.[9, 10] Measurements were obtained at 3 different points on either side of the vessel.

Isobaric tone of isolated cerebral arteries

A segment of middle cerebral artery was dissected and cannulated using glass micro cannulas, and mounted in a pressure myograph (111P, DMT), as described previously.[11] Experiments were performed under no-flow conditions. Arteries were equilibrated at 37°C and pressure was cycled between 10 and 120 mmHg to decrease mechanical hysteresis. Vessel diameter was measured from video images using contrast analysis (DMT Vessel Acquisition Suite, DMT), with arteries being subjected to a series of pressure steps (20, 40, 60, 80 and 100 mmHg), with 3 minutes intervals. The diameter was measured for at last 30 seconds in a 3 minute interval. The pressure-step protocol was repeated for arteries under control conditions in PSS, and after 15 minutes incubation in Ca^{2+}-free PSS in the presence of 30 µM papaverine and 10 µM Y27632. The outer diameters obtained under these conditions were considered active (AD) and passive diameters (PD), respectively. The degree of tone at each pressure level was quantified as [1 - (AD / PD)].

Laser speckle analysis

Laser speckle (LS) imaging experiments were performed in order to assess resting blood flow through cerebral arteries *in vivo* (Fig. 1A and Suppl. Fig. 1A). A segmentation algorithm[12, 13] was applied to the arteries (Suppl. Fig. 1B) that were identified as major branches of the middle cerebral artery (Suppl. Fig. 1A). The segmentation algorithm was applied to extract diameter and corresponding speckle contrast values for selected arteries (Suppl. Fig. 1B). These values were then averaged over the artery segment and used to estimate volumetric blood flow dynamics (blood flow index).

Mice were anaesthetised by a subcutaneous injection of ketamine (80 mg/kg ; Ketaminol®vet, Intervet International, Boxmeer, The Netherlands) and xylazine (8 mg/kg; Narcoxyl®vet, Intervet International). Mice were placed on a thermostatic platform with the head fixed in a stereotaxic frame. Hairs on the scalp were trimmed, and the skin and periost removed to expose the skull. Images were taken with an intact skull, i.e. no craniotomy was applied.

Coherent infrared light was provided by an LDM785 laser unit, controlled by the diode driver CLD1011LP (Thorlabs Inc., Newton, NJ, USA). The laser light was directed to the cranial surface and the speckle signal was recorded by a CMOS camera (acA2000-165umNIR; Basler AG, Ahrensburg, Germany) mounted on the video lens (VZM 200i, Edmund Optics, USA). Laser power density was set to ~10 mW cm^{-2}.[14]

Chemicals

The sequence of pNaKtide is GRKKRRQRRRPPQSATWLALSRIAGLCNRAVFQ [15]. This peptide is composed of 20 amino acids from the N–domain of the Na,K-ATPase and a leader peptide sequence of 13 amino acids that allows cell membrane penetration. The pNaKtide is water soluble and prior studies have shown that it is effective in blocking the Na,K-ATPase-dependent cSrc activation [15-20]. Stock pNaKtide solution (HD Biosciences, China; purity >95%) was prepared in water (10^{-2} M) and stored at -20°C. pNaKtide was applied at least 15 minutes prior to interventions.

Ouabain stock solution (10^{-2} M) was prepared in water and stored at 4°C for a maximum 1 week. All other stocks were stored at -20°C before use. PP2 (10^{-2} M) and digoxin (10^{-2} M) stock solutions were prepared in dimethylsulfoxid (DMSO). U46619 (10^{-2} M) was dissolved in ethanol. Endothelin-1(10^{-3} M) was dissolved in water and 1% acetic acid. Noradrenaline (10^{-2} M) and phentolamine (10^{-3} M) were dissolved in water. U46619 was from Tocris Bioscience, UK; all other chemicals were from Sigma Aldrich, Denmark.

Data analyses

Microsoft Excel and GraphPad Prism software (v.5.02) were used for graphing and statistical analysis. Data are summarized as the mean value ± SEM of the sample group. Sample size was calculated in order to detect a minimum difference of 25% (standard deviation) within any measurement with a 5% error and have a power of 0.8. Concentration-response curves were fitted to experimental data using four-parameter, non-linear regression curve fitting. From these curves, pD_2 (-log to the concentration required to produce a half-maximal response), the Hill slope and maximal response were derived and compared using an extra sum-of-squares *F* test to assess the overall significance for a regression model.[21, 22] Area under the dose-response curve (AUC) was calculated based on trapezoidal rule. Significant differences between means were determined by either one-way or two-ways ANOVA, where appropriate, followed by Bonferroni correction for multiple comparison or by Student t-test. A probability (*P*) level of <0.05 was considered significant and *n* refers to number of rats.

SUPPLEMENTARY FIGURES

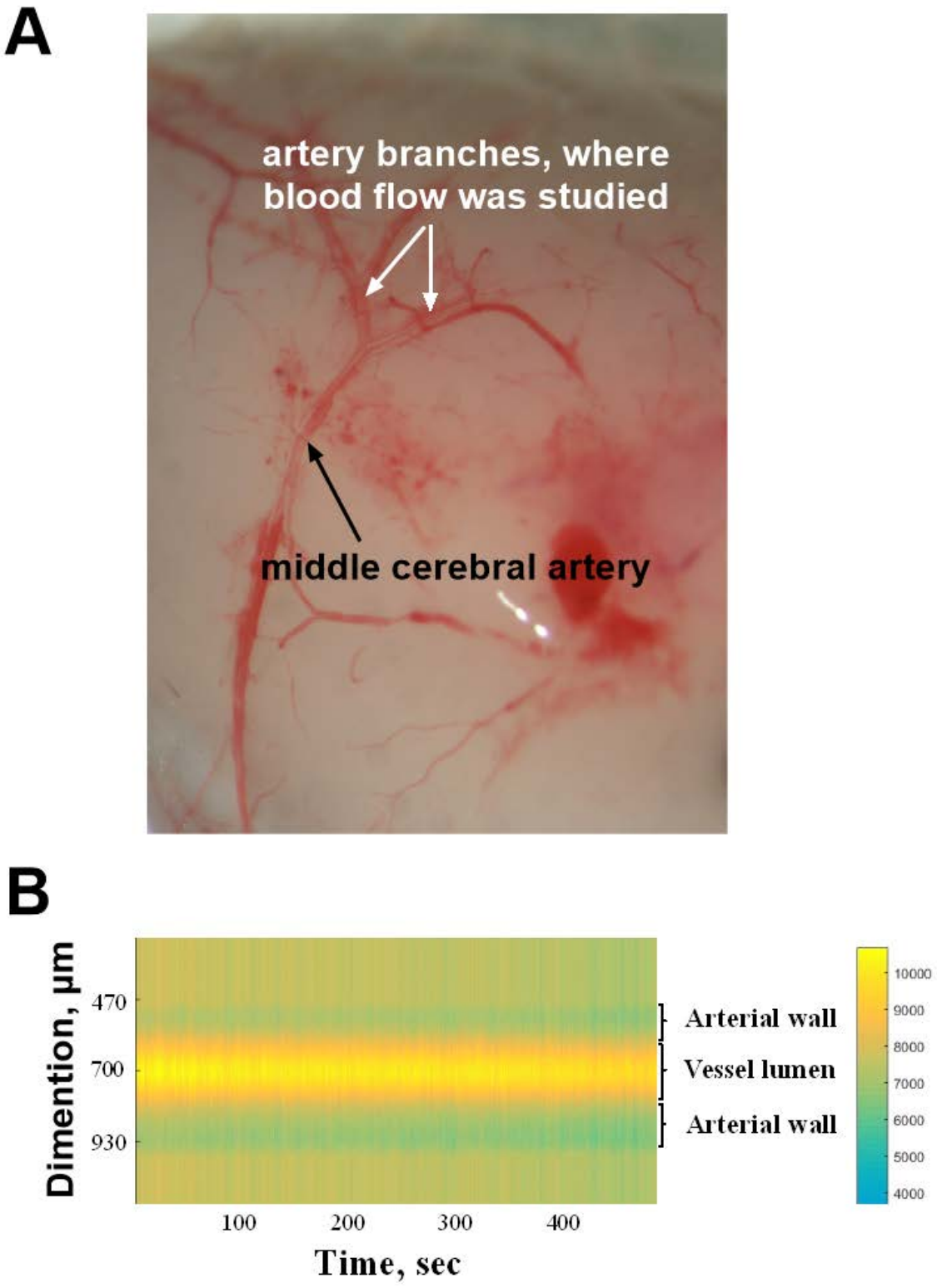

Supplementary Figure 1. **Laser Speckle imaging of mouse middle cerebral artery diameter and blood flow *in vivo*.** Representative post-mortem brain image showing murine middle cerebral artery (black arrow) and its branches (white arrows), from which diameter and blood flow index were estimated by Laser Speckle analysis (A). A single artery segmentation profile (B). Average vessel dimensions (Y-axis) are calculated from the region of interest and plotted as a function of time (X-axis). An area with low velocity around the lumen was identified as the arterial wall whereas the area with high velocity was determined as the lumen.[12, 13]

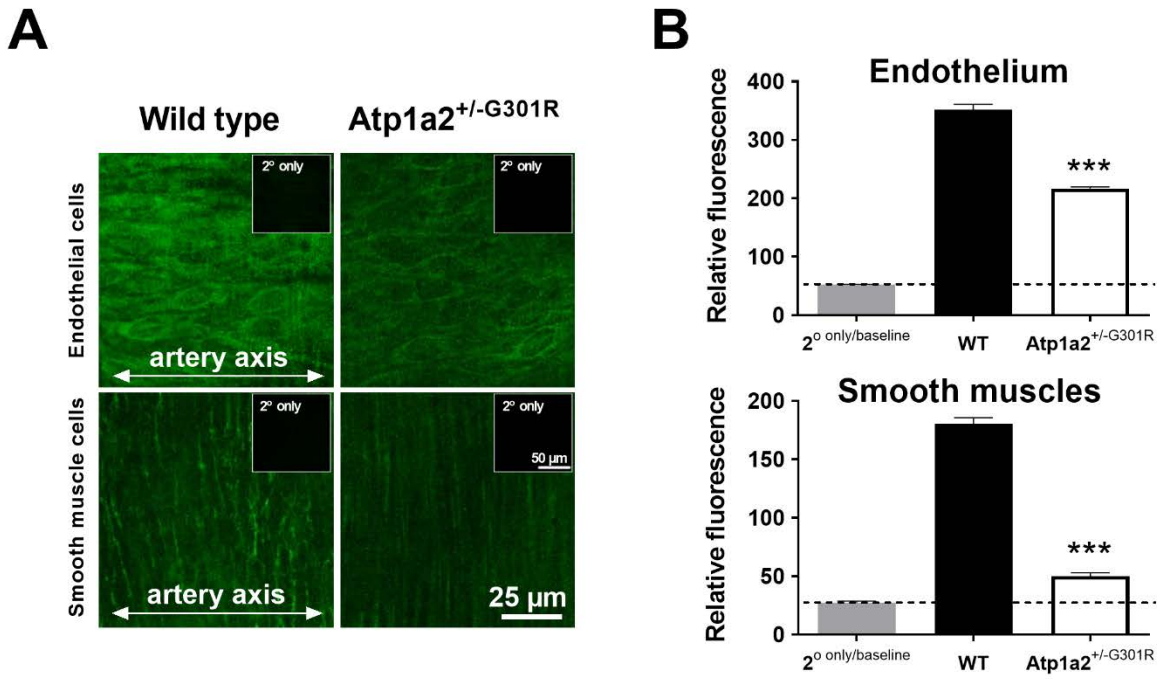

Supplementary Figure 2. Confocal imaging and semi-quantitative fluorescence density of NCX protein. Middle cerebral arteries from the Atp1a2$^{+/-G301R}$ mice have decreased NCX protein expression. Representative (A) and averaged (B) results of whole-mount staining (n=4). *** indicates P<0.001 in comparison with WT (one-way ANOVA).

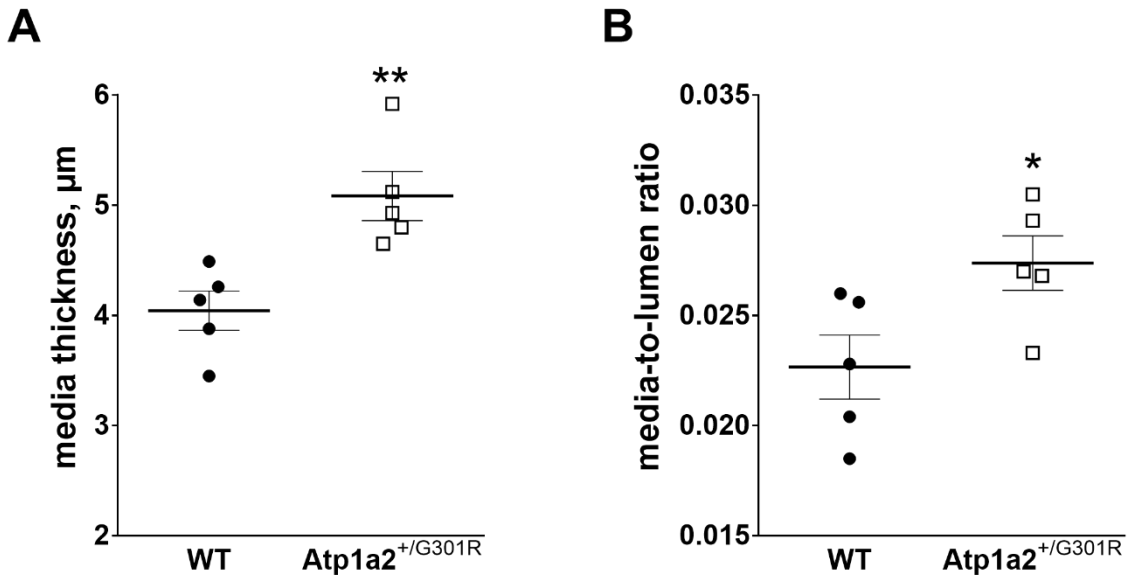

Supplementary Figure 3. Middle cerebral arteries from Atp1a$^{2+/-G301R}$ mice have increased media thickness and media-to-lumen ratio. Morphological measurements of middle cerebral arteries found an increased media thickness (A) and media-to-lumen ratio (B) of arteries from Atp1a$^{2+/-G301R}$ mice in comparison with WT. *n*=5. * and ** indicate *P*<0.05 and <0.01.

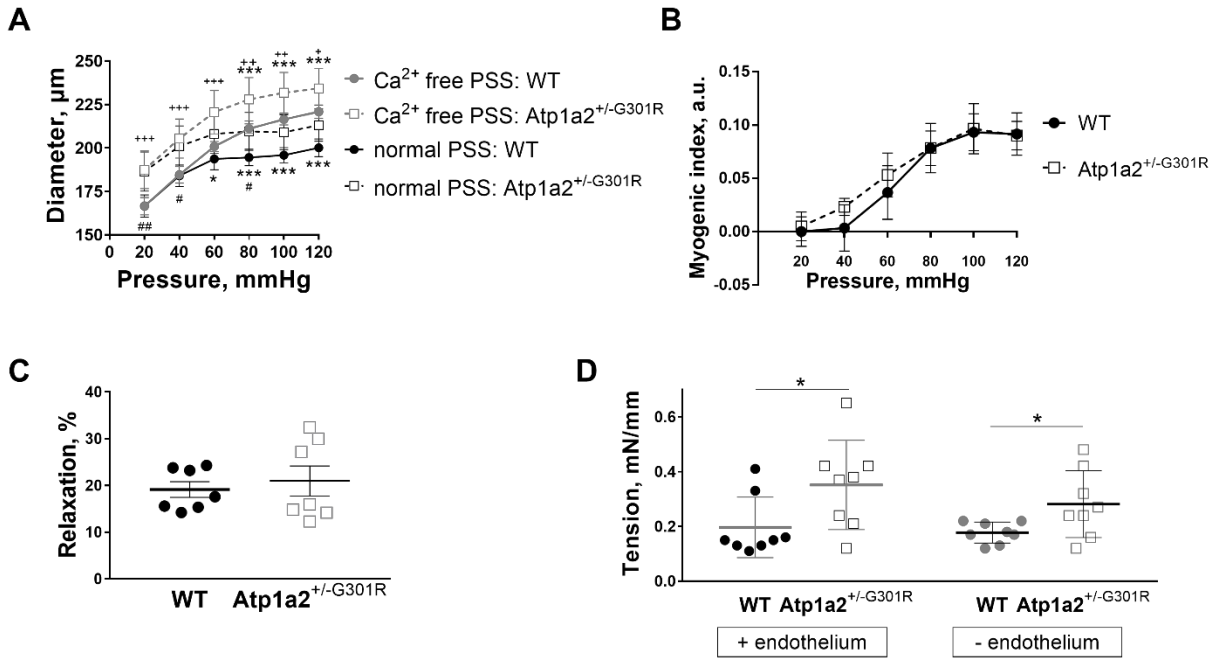

Supplementary Figure 4. Middle cerebral arteries from Atp1a$^{2+/-G301R}$ mice have unchanged myogenic tone and endothelium-dependent relaxation to ACh, while they constricted stronger than WT to agonist stimulation independent of the endothelium.

A. Middle cerebral arteries from Atp1a$^{2+/-G301R}$ and WT mice were exposed to different transmural pressures from 20 to 120 mmHg under control conditions in normal physiological salt solution (PSS), and fully relaxed in Ca^{2+}-free PSS with $3x10^{-5}$ M papaverine and 10^{-5} M Y27632. +,++ and +++ indicate P<0.05, <0.01 and <0.001 for comparison between Atp1a$^{2+/-G301R}$ and WT group in Ca^{2+} free PSS; # and ## indicate P<0.05 and <0.01 for comparison between Atp1a$^{2+/-G301R}$ and WT group in normal PSS; * and *** indicate P<0.05 and <0.001 for comparison of the same arteries in Ca^{2+} free and normal PSS (one-way ANOVA). n=6.

B. Myogenic tone expressed as a myogenic index at each pressure level, e.g. [1 - (arterial diameter in normal PSS / arterial diameter in Ca^{2+} free PSS)] shown in A. No difference between cerebral arteries from Atp1a$^{2+/-G301R}$ and WT mice was seen. n=6.

C - Middle cerebral arteries from Atp1a$^{2+/-G301R}$ and WT mice were pre-constricted with U46619 (~50% of maximal tone) and relaxed with ACh (10^{-5} M). No difference in endothelium-dependent relaxation was seen between the groups. *n*=7.

D – Endothelium-intact and endothelium-denuded middle cerebral arteries from Atp1a$^{2+/-G301R}$ and WT mice were constricted with U46619 (10^{-5} M), as indicated. * shows $P<0.05$. *n*=8.

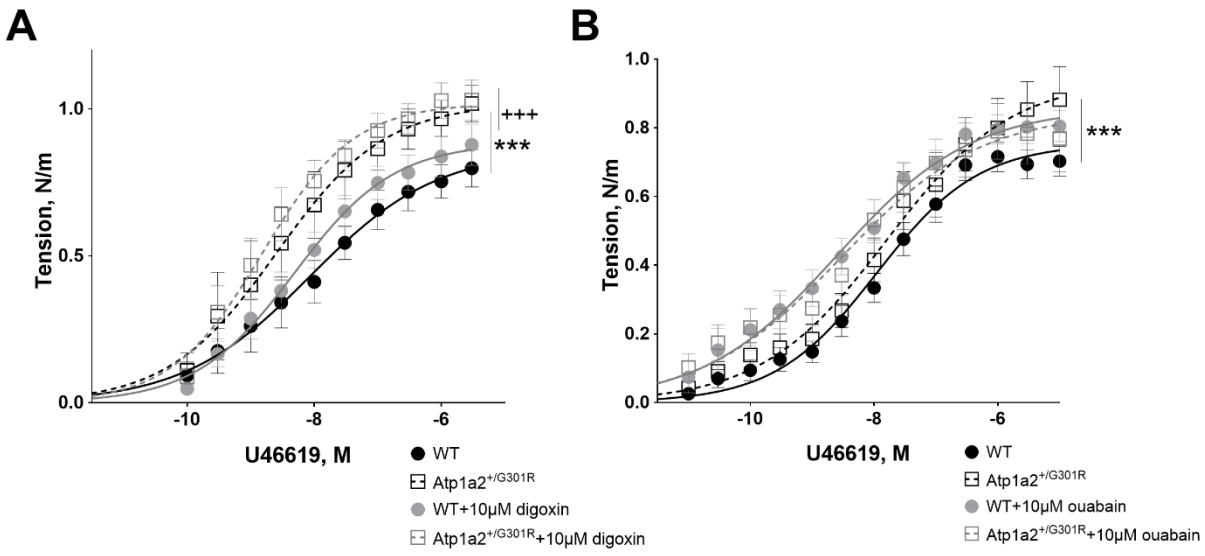

Supplementary Figure 5. Ouabain, but not digoxin, abolishes the difference in contractile response of middle cerebral arteries from Atp1a2$^{+/-G301R}$ and WT mice. Digoxin (10 μM) was without significant effect on the constriction of arteries from WT and Atp1a2$^{+/-G301R}$ (A; *n*=6). The contractile responses of cerebral arteries from Atp1a2$^{+/-G301R}$ mice were significantly stronger in comparison with WT before (*P*<0.001; ***) and after pre-treatment with digoxin (*P*<0.001; +++). Ouabain (10 μM) abolished the significant difference in contractile responses between arteries from Atp1a2$^{+/-G301R}$ and WT seen under control conditions (B; ***, *P*<0.001; *n*=10).

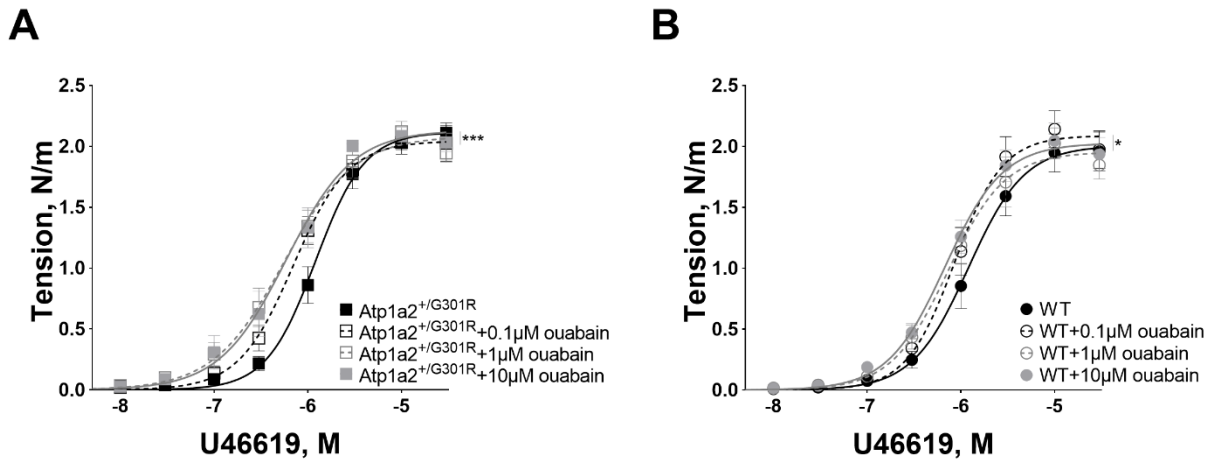

Supplementary Figure 6. Ouabain potentiated constriction to U46619 of mesenteric small arteries from both Atp1a2$^{+/-G301R}$ and WT mice to the same extent. Ouabain significantly potentiated constriction of mesenteric small arteries from the Atp1a2$^{+/-G301R}$ (A; ***, P<0.001) and WT mice (B; *, P<0.05) at 0.1 μM concentration, and no further potentiation was seen at 1 and 10 μM ouabain.

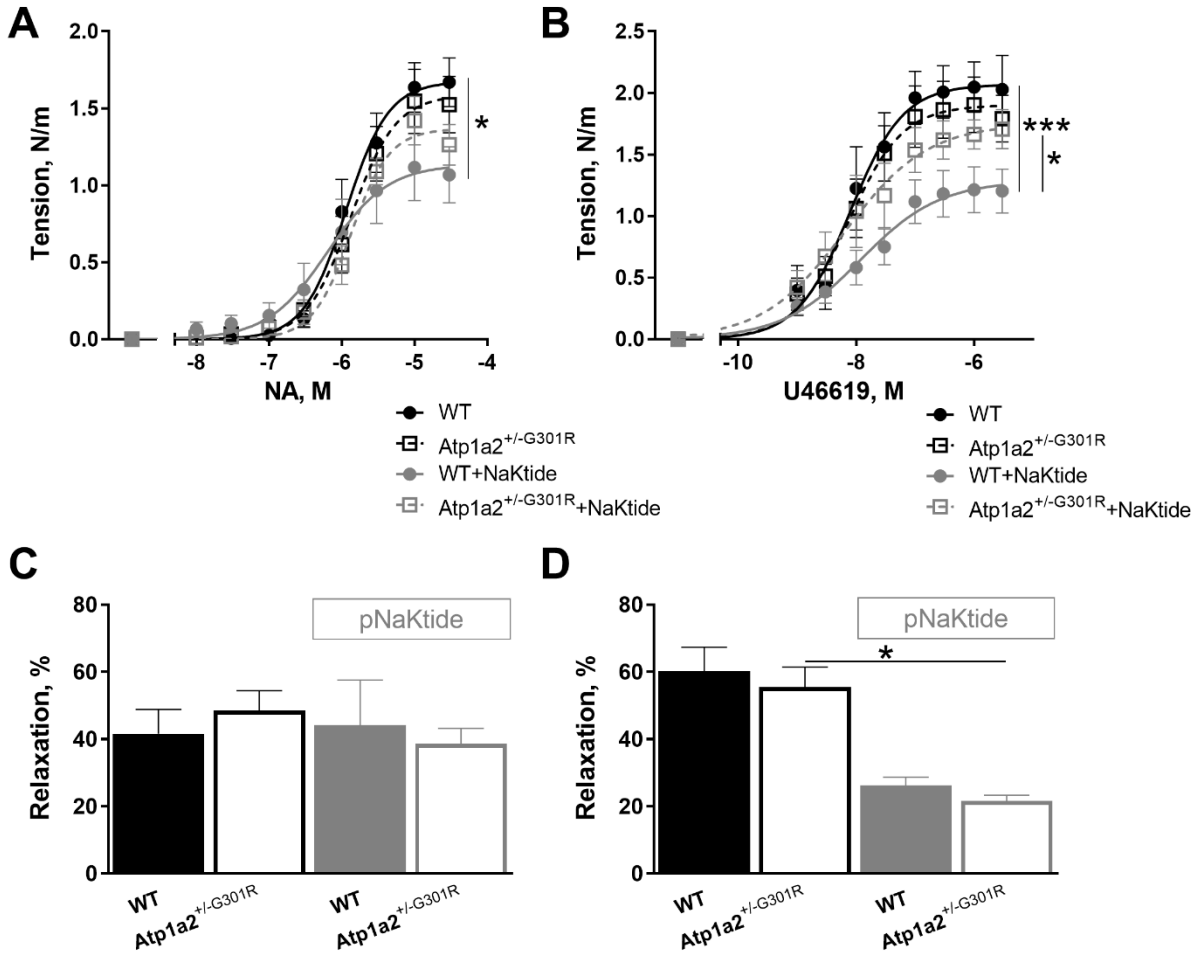

Supplementary Figure 7. No difference in agonist-induced constriction and endothelium-dependent relaxation of mesenteric small arteries from Atp1a2$^{+/-G301R}$ and WT mice. Under control conditions (*n*=8), contractile responses to NA were similar for arteries from Atp1a2$^{+/-G301R}$ and WT mice (A). Pre-incubation with 2 µM pNaKtide significantly (*, *P*<0.05) suppressed constriction of arteries from WT (*n*=5), but was without any effect on arteries from Atp1a2$^{+/-G301R}$ (*n*=6). U46616 induced similar contractile responses in two groups under control conditions (B; *n*=8). pNaKtide significantly (***, *P*<0.001) suppressed constriction of arteries from WT leading to differences (***, *P*<0.001; *n*=6) between arteries from WT and Atp1a2$^{+/-G301R}$ in the presence of pNaKtide. ACh-induced relaxation of arteries pre-constricted with 3 µM NA from Atp1a2$^{+/-}$

^{G301R} (*n*=14) and WT mice (*n*=13) in response to 3 µM (C) and 10 µM (D) ACh. Experiments were performed under control conditions (*n*=13-14) and in the presence of 2 µM pNaKtide (*n*=3-4). pNaKtide significantly (*; $P<0.05$) suppressed the relaxation to 10 µM ACh (D).

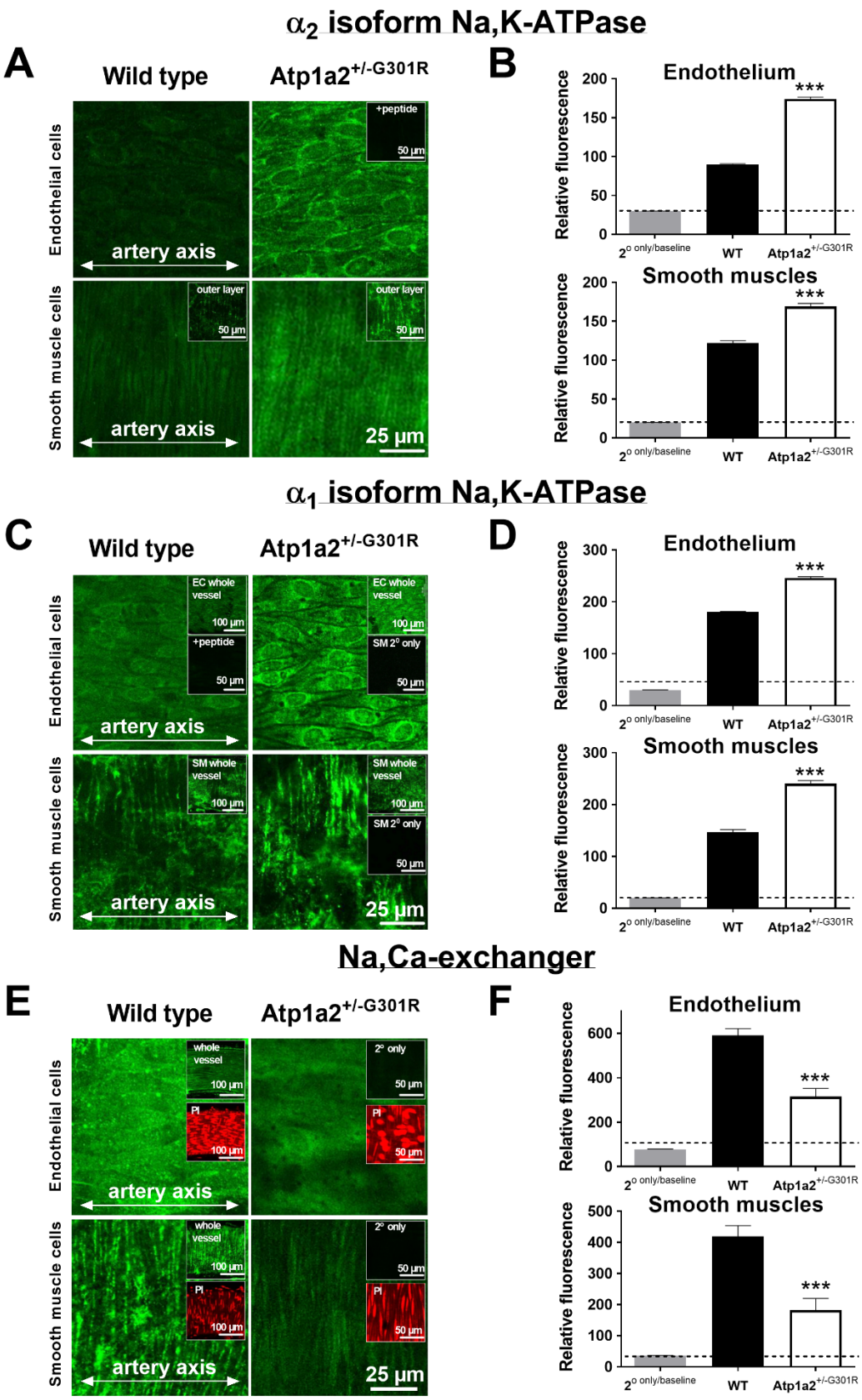
α2 isoform Na,K-ATPase
A
Wild type
Atp1a2+/-G301R
Endothelial cells
Smooth muscle cells
+peptide
50 µm
artery axis
outer layer
25 µm
B
Endothelium
Relative fluorescence
***
2° only/baseline
WT
Atp1a2+/-G301R
Smooth muscles
α1 isoform Na,K-ATPase
C
EC whole vessel
100 µm
SM 2° only
SM whole vessel
D
Na,Ca-exchanger
E
whole vessel
2° only
PI
F

Supplementary Figure 8. Confocal imaging and semi-quantitative fluorescence density of α1/2 isoform Na,K-ATPase and NCX protein. Mesenteric small arteries from Atp1a2$^{+/-G301R}$ mice have increased expression of Na,K-ATPase α_2 (A, B) and α_1 isoform (C, D) protein. Representative images from whole–mount immunostaining for the α_2 (A) and α_1 isoform (C), with semi-quantitative fluorescence (B, D, respectively; *n*=5). Mesenteric small arteries from the Atp1a2$^{+/-G301R}$ mice had decreased NCX protein expression in both smooth muscle and endothelial cells; representative (E) with semi-quantitative fluorescence (F; *n*=4). *** indicates *P*<0.001 vs. WT (one-way ANOVA).

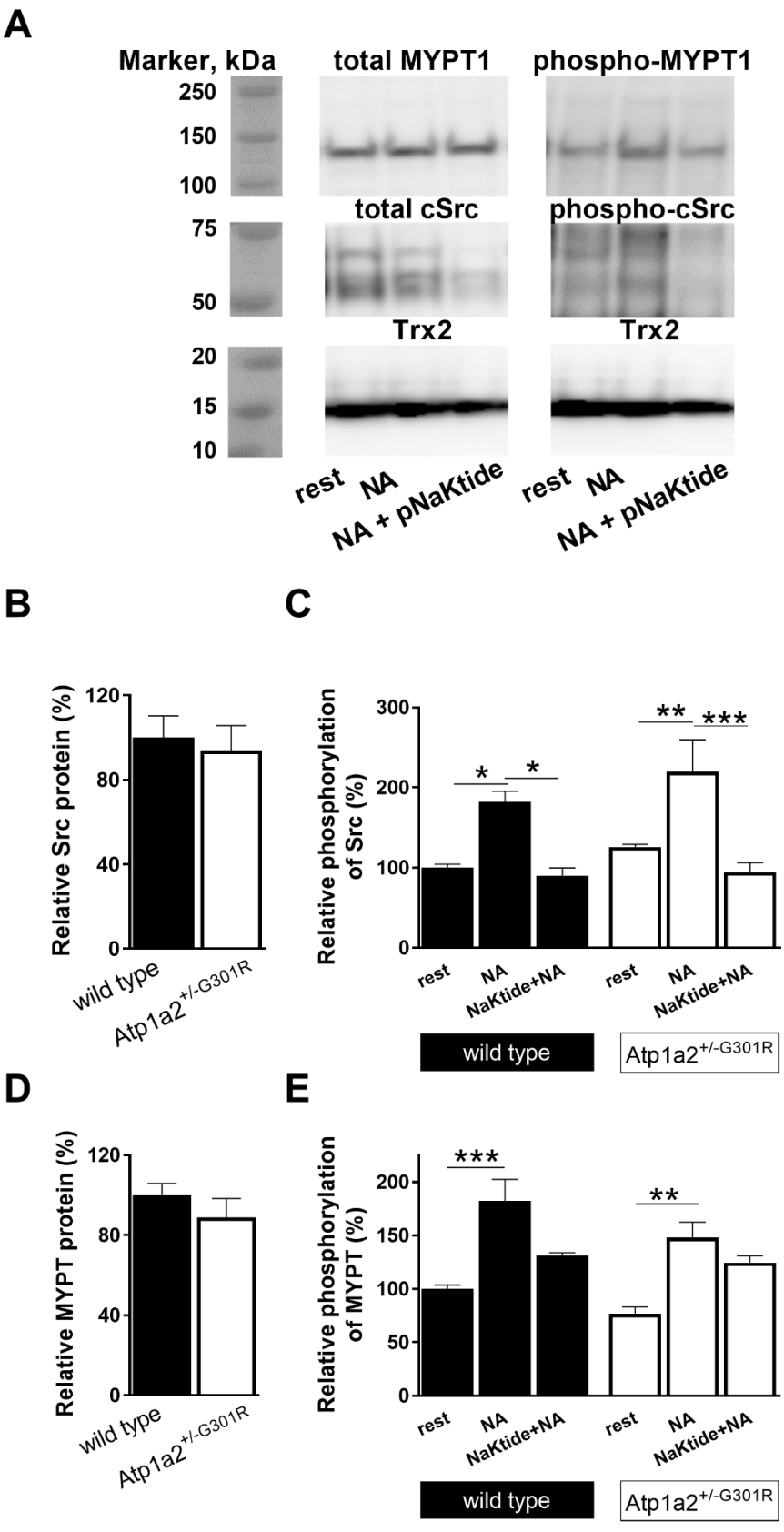
A
Marker, kDa
total MYPT1
phospho-MYPT1
250
150
100
total cSrc
phospho-cSrc
75
50
Trx2
Trx2
20
15
10
rest
NA
NA + pNaKtide
rest
NA
NA + pNaKtide
B
Relative Src protein (%)
120
80
40
0
wild type
Atp1a2+/-G301R
C
Relative phosphorylation of Src (%)
300
200
100
0
*
*
**
***
rest
NA
NaKtide+NA
rest
NA
NaKtide+NA
wild type
Atp1a2+/-G301R
D
Relative MYPT protein (%)
120
80
40
0
wild type
Atp1a2+/-G301R
E
Relative phosphorylation of MYPT (%)
200
150
100
50
0
***
**
rest
NA
NaKtide+NA
rest
NA
NaKtide+NA
wild type
Atp1a2+/-G301R

Supplementary Figure 9. Expression and phosphorylation of cSrc kinase and MYPT1 in mesenteric small arteries from Atp1a2$^{+/-G301R}$ and WT mice. Arteries were treated with 10 μM NA either under control conditions or after pre-treatment with 2 μM pNaKtide, as indicated. Representative Western blot where expression and phosphorylation of cSrc and MYPT1 (in WT mesenteric arteries; A). Thioredoxin2 (Trx2) was used as loading control. No difference in the expression of total Src kinase (normalized to Trx2 band density) was seen between the groups (B; *n*=14-15). U46619 stimulation increased cSrc phosphorylation in both groups and this was abolished by pNaKtide (C; *n*=6-14) (calculated as a ratio of phosphorylated and total cSrc, normalised to averaged values for WT under resting conditions). Total expression (D) and phosphorylation of MYPT1 at Thr-850 (E) were the same for two groups under resting conditions (*n*=6-8). NA significantly elevated MYPT1 phosphorylation (*n*=6-8), but pNaKtide partially reduced MYPT1 phosphorylation (*n*=5-7). *, ** and ***, $P<0.5$, <0.01 and <0.001 vs. WT (2-way ANOVA).

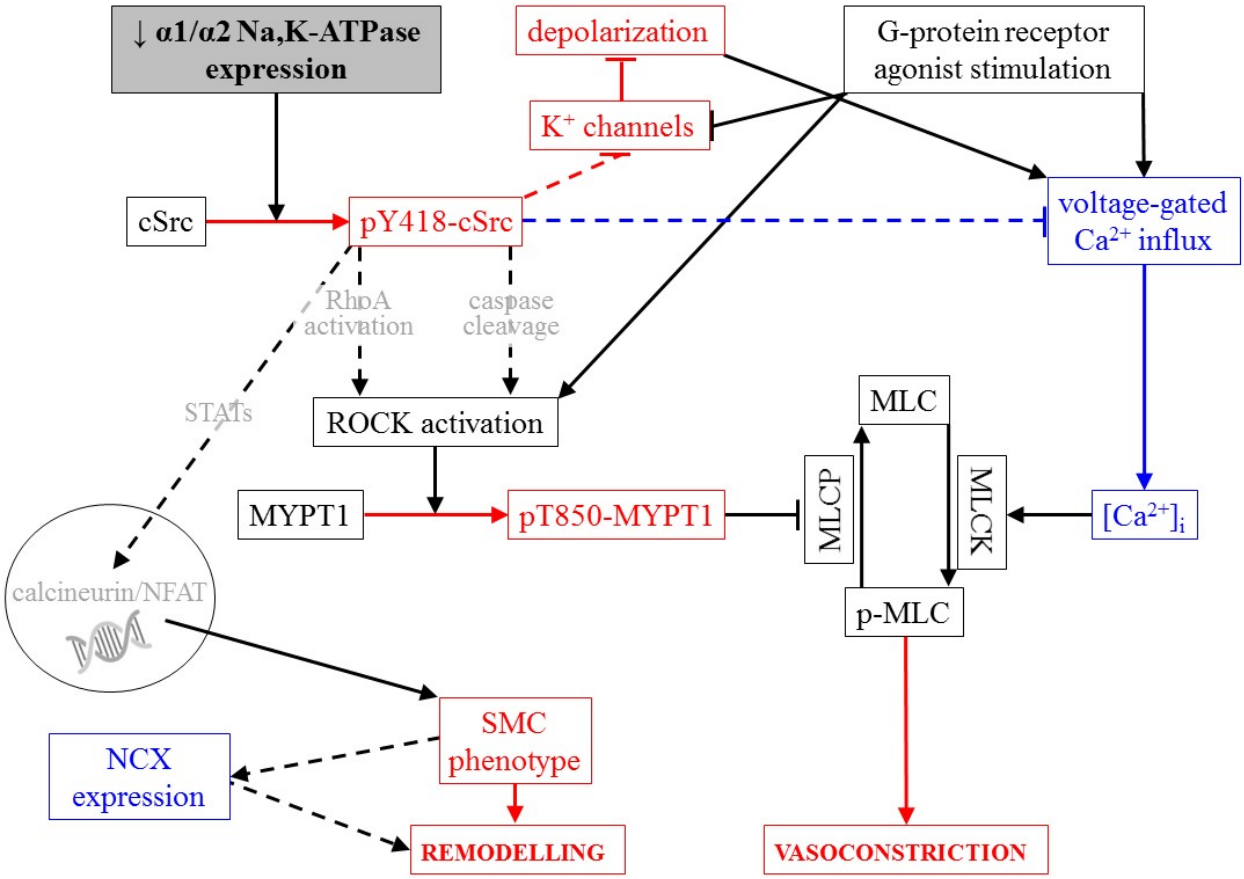

Supplementary Figure 10. Reduced expression of the Na,K-ATPase in the Atp1a2$^{+/-G301R}$ mice modulates several signalling pathways in smooth muscle cells and leads to enhanced cerebral artery tone and remodelling. A schematic presentation of the pathways suggested involved, where upregulated signalling in Atp1a2$^{+/-G301R}$ mice is shown in red, and downregulated signalling in blue. Hypothetical interactions are indicated by 'dashed' lines. The present study demonstrates that reduced Na,K-ATPase expression is associated with phosphorylation of cSrc kinase leading to myosin phosphatase targeting protein 1 (MYPT1) phosphorylation, smooth muscle sensitization to Ca^{2+} and potentiated vasoconstriction. The mechanism for cSrc-dependent Rho-associated kinase (ROCK) activation is unclear and might involve either potentiation of RhoA signalling[23] or ROCK cleavage by caspase.[24] Despite stronger agonist-induced depolarization of

smooth muscle cells from Atp1a2$^{+/-G301R}$ mice, reduced voltage-dependent Ca^{2+} influx was seen, supporting the suggestion that potentiated vasoconstriction is a result of Ca^{2+} sensitization. Tyrosine phosphorylation of signal transducers and activators of transcription (STATs)[25] or changes in $[Ca^{2+}]_i$ homeostasis[26] can modulate the activity of nuclear expression factors, e.g. calcineurin/NFAT pathway, and affect vascular smooth muscle phenotype leading to arterial remodelling.

References

1. Bottger P, Glerup S, Gesslein B, et al. Glutamate-system defects behind psychiatric manifestations in a familial hemiplegic migraine type 2 disease-mutation mouse model. *Sci Rep* 2016; 6: 22047. DOI: 10.1038/srep22047.

2. Yan Y and Shapiro JI. The physiological and clinical importance of sodium potassium ATPase in cardiovascular diseases. *Curr Opin Pharmacol* 2016; 27: 43-49. DOI: 10.1016/j.coph.2016.01.009.

3. Isaksen TJ and Lykke-Hartmann K. Insights into the Pathology of the alpha2-Na(+)/K(+)-ATPase in Neurological Disorders; Lessons from Animal Models. *Front Physiol* 2016; 7: 161. DOI: 10.3389/fphys.2016.00161.

4. Friedrich T, Tavraz NN and Junghans C. ATP1A2 Mutations in Migraine: Seeing through the Facets of an Ion Pump onto the Neurobiology of Disease. *Front Physiol* 2016; 7: 239. DOI: 10.3389/fphys.2016.00239.

5. Gage GJ, Kipke DR and Shain W. Whole animal perfusion fixation for rodents. *J Vis Exp* 2012; 65. DOI: 10.3791/3564.

6. Mulvany MJ and Halpern W. Contractile properties of small arterial resistance vessels in spontaneously hypertensive and normotensive rats. *Circ Res* 1977; 41: 19-26.

7. Jensen PE, Mulvany MJ and Aalkjaer C. Endogenous and exogenous agonist-induced changes in the coupling between $[Ca^{2+}]_i$ and force in rat resistance arteries. *Pflügers Arch* 1992; 420: 536-543.

8. Matchkov VV, Rahman A, Bakker LM, et al. Analysis of effects of connexin-mimetic peptides in rat mesenteric small arteries. *Am J Physiol* 2006; 291: H357-H367.

9. Mulvany MJ, Hansen OK and Aalkjaer C. Direct evidence that the greater contractility of resistance vessels in spontaneously hypertensive rats is associated with a narrowed lumen, a thickened media, and an increased number of smooth muscle cell layers. *Circ Res* 1978; 43: 854-864.

10. Kudryavtseva O, Herum KM, Dam VS, et al. Downregulation of L-type Ca2+ channel in rat mesenteric arteries leads to loss of smooth muscle contractile phenotype and inward hypertrophic remodeling. *Am J Physiol Heart Circ Physiol* 2014; 306: H1287-1301. DOI: 10.1152/ajpheart.00503.2013.

11. Matchkov VV, Moeller-Nielsen N, Secher D, V, et al. The alpha2 isoform of the Na,K-pump is important for intercellular communication, agonist-induced contraction and EDHF-like response in rat mesenteric arteries. *Am J Physiol* 2012; 303: H36-H46.

12. Postnov DD, Tuchin, V.V. and Sosnovtseva O. . Estimation of vessel diameter and blood flow dynamics from laser speckle images. *Biomedical Optics Express* 2016; 7: 10. 22 Jun 2016. DOI: 10.1364/BOE.7.002759.

13. Nyvad J, Mazur A, Postnov DD, et al. Intravital investigation of rat mesenteric small artery tone and blood flow. *J Physiol* 2017; 595: 5037-5053. 2017/06/02. DOI: 10.1113/JP274604.

14. Postnov DD, Sosnovtseva O and Tuchin VV. Improved detectability of microcirculatory dynamics by laser speckle flowmetry. *J Biophotonics* 2015.

15. Li Z, Cai T, Tian J, et al. NaKtide, a Na/K-ATPase-derived peptide Src inhibitor, antagonizes ouabain-activated signal transduction in cultured cells. *J Biol Chem* 2009; 284: 21066-21076.

16. Sodhi K, Maxwell K, Yan Y, et al. pNaKtide inhibits Na/K-ATPase reactive oxygen species amplification and attenuates adipogenesis. *Sci Adv* 2015; 1: e1500781. DOI: 10.1126/sciadv.1500781.

17. Hangaard L, Bouzinova EV, Staehr C, et al. Na,K-ATPase regulates intercellular communication in the vascular wall via cSrc kinase dependent connexin43 phosphorylation. *Am J Physiol* 2017: ajpcell 00347 02016. DOI: 10.1152/ajpcell.00347.2016.

18. Xie J, Ye Q, Cui X, et al. Expression of Rat Na/K-ATPase alpha2 Enables Ion Pumping but not Ouabain-Induced Signaling in alpha1-Deficient Porcine Renal Epithelial Cells. *Am J Physiol* 2015; 309: C373-382. 2015 Jun 24. DOI: 10.1152/ajpcell.00103.2015.

19. Lai F, Madan N, Ye Q, et al. Identification of a Mutant alpha1 Na/K-ATPase That Pumps but Is Defective in Signal Transduction. *J Biol Chem* 2013; 288: 13295-13304.

20. Li Z, Zhang Z, Xie JX, et al. Na/K-ATPase mimetic pNaKtide peptide inhibits the growth of human cancer cells. *J Biol Chem* 2011; 286: 32394-32403.

21. Kenakin TP. *A pharmacology primer: theory, application, and methods.* 3rd ed. Burlington, MA, USA: Elsevier Inc., 2009.

22. Motulsky H and Christopoulos A. *Fitting models to biological data using linear and nonlinear regression. A practical guide to curve fitting.* San Diego CA: GraphPad Software, Inc., 2003.

23. Suzuki N, Nakamura S, Mano H, et al. Galpha 12 activates Rho GTPase through tyrosine-phosphorylated leukemia-associated RhoGEF. *Proc Natl Acad Sci U S A* 2003; 100: 733-738. DOI: 10.1073/pnas.0234057100.

24. Ark M, Ozdemir A and Polat B. Ouabain-induced apoptosis and Rho kinase: a novel caspase-2 cleavage site and fragment of Rock-2. *Apoptosis* 2010; 15: 1494-1506. 2010/07/28. DOI: 10.1007/s10495-010-0529-1.

25. MacKay CE and Knock GA. Control of vascular smooth muscle function by Src-family kinases and reactive oxygen species in health and disease. *J Physiol* 2015; 593: 3815-3828. DOI: 10.1113/jphysiol.2014.285304.

26. Kudryavtseva O, Aalkjaer C and Matchkov VV. Vascular smooth muscle cell phenotype is defined by Ca(2+) -dependent transcription factors. *FEBS J* 2013; 280: 5488-5499.